Viola-Seaborg relation for α-decay half-lives: Update and microscopic determination of parameters

Basudeb Sahu[1] and Swagatika Bhoi[2]
[1]*Department of Physics, College of Engineering and Technology, Bhubaneswar 751003, India*
[2]*Department of Physics, Jyotivihar, Sambalpur University, Burla, 768019, India*

(Received 25 October 2015; revised manuscript received 10 February 2016; published 1 April 2016)

Considering the emission process of α particles in the transition from an isolated quasibound state to a scattering state, a clear expression for the decay width derived in terms of regular Coulomb function, the quasibound state wave function, and the difference of potentials is analyzed. The Schrödinger equation with the effective potential representing the α + nucleus interaction consistent with the potential obtained in the relativistic mean-field approximation is solved exactly for the wave function. Using this exact wave function at resonance and the difference of the above potential from the point charge Coulomb interaction in the expression of decay width stated above, an analytic expression for the decay half-life is derived from the width. By invoking some approximations for different functions in this expression, a closed formula for the logarithm of half-life in terms of characteristic Q value equal to the resonance energy and the mass and charge numbers of the α emitter is obtained. The calculated results of half-life obtained by using the analytic expression of half-life or the closed formula for the logarithm of the half-life are shown to explain the corresponding measured data with values ranging from 10^{-6} s to 10^{22} y in the case of large numbers of α emitters that include heavy and superheavy nuclei. The results of the closed formula aligned in a straight line closely explain the rectilinear arrangement of the logarithm values of experimental results for decay half-lives as a function of a quantity that depends on Q values and charge numbers of the emitters. The analytic closed formula with all its terms defined is preferable to the empirical Viola-Seaborg rule of α-decay rate.

DOI: 10.1103/PhysRevC.93.044301

I. INTRODUCTION

With the discovery of a number of α-particle emitters including heavy and superheavy nuclei with proton numbers as large as 118 and observations of decay rates as large as 10^{22} y, corresponding to very narrow width of the order of 10^{-50} MeV, the interpretation of α radioactivity has become of theoretical interest. In 1928, Gamow [1] tried to apply quantum mechanics to the process of α decay and explained it as a quantum tunneling effect. The empirical law of Geiger and Nuttall (GN) [2] could be explained by this calculation.

Many other semiempirical relationships for α decay rate of heavy and superheavy elements have also been developed where one finds mostly the use of the semiclassical approximations like the Wentzel-Kramers-Brillouin (WKB) method for the tunneling of a potential barrier [3–8].

A large body of experimental and theoretical findings about the α-decay mode has been covered extensively in Refs. [9–17].

The logarithm of the experimental results of decay half-lives, $T_{1/2}$, of large body of α emitters with $Z = 54$–118 is plotted as a function of the Coulomb parameter $\chi = Z_\alpha Z_D\sqrt{\frac{A_\alpha A_D}{(A_\alpha+A_D)Q_\alpha}}$, as done in the GN law, with Q_α representing the α-decay energy, A_α and A_D denoting mass numbers, and Z_α and Z_D denoting charge numbers of the α particle and the daughter nucleus, respectively. It is found [18] that the experimental data do not fall in a single linear path but are diffused or aligned in several linear segments with different slopes and intercepts. The GN law, usually designed for a single straight line for all α emitters, fails to address this manifestation of the data. However, if the same experimental results in logarithm form are plotted as a function of the Viola-Seaborg parameter [18], $\tilde{V} = \frac{a'Z_D+b'}{\sqrt{Q_\alpha}} + c'Z_D$, where a', b', and c' are constants, the data align themselves in a narrow linear path. The empirical Viola-Seaborg (VS) rule [18,19], $\log_{10}T_{1/2} = \frac{a'Z_D+b'}{\sqrt{Q_\alpha}} + c'Z_D + d'$ with $a' = 1.478$, $b' = 8.714$, $c' = -0.183$, and $d' = -34.699$, is successful in accounting for the above variation of the measured data. Looking to the success of this formulation, we become curious whether a formula of logarithm of half-lives in terms of well-defined parameters or coefficients can be derived on the basis of the fundamental principle of decay when the empirical nature of the VS rule is removed.

Because in a heavy nucleus the shell-model states are highly mixed and α clustering is in evidence for heavy and superheavy nuclei [20], the calculation of the decay width is significantly simplified by the premise of the existence of a preformed α particle. Hence, the many-body problem of α decay from a nucleus can be considered a two-body problem composed of the daughter nucleus plus an α particle. The fundamental R-matrix theory, being the mechanics of a two-body problem, can be applicable to describe the initial system of α + daughter nucleus connected with the instability of the quasibound or resonance state of the decaying nucleus. Most recently Qi *et al.* [21–23] have tried to include the tunneling process in the R-matrix theory and proposed an extended version of the GN rule. The R-matrix theory, which is a three-dimensional potential scattering problem, cannot be simply represented or converted to a one-dimensional process for tunneling of the potential barrier without using changes in the potential. The potential suitable for the description of the scattering phenomenon may not be sufficient to give the expected result of width of decay within the tunneling model using a semiclassical WKB approximation for calculating the transmission coefficient. This is exactly what happens in the case of cosh-shaped potential [12] where the height of the barrier is increased artificially to suit the calculation of width in the semiclassical WKB method. As rightly pointed out by Mohr [24], in principle, the application of a semiclassical model is not necessary for the calculation of α-decay half-life or width.

The fundamental R-matrix theory for the decay of a cluster or particle can be fully visualized in terms of the S-matrix theory of resonance scattering or the transition scattering from an isolated quasibound state to a scattering state. The S-matrix method treats resonance as a pole in the complex energy plane with its real part representing resonance energy or the Q-value of decay and the imaginary part of the decay half-life. In the latter picture, the decay width is a resonance width in the system consisting of an α cluster and the residual nucleus.

One can estimate the values of resonance energy and the width of decay from the rapidly rising scattering phase shift δ_ℓ with momentum or energy over a range of angle π [24]. It requires a Breit-Wigner one-level approximation for the resonances corresponding to an increase of phase shift across $\frac{\pi}{2}$. However, as rightly pointed out by Mohr [24], this method is difficult to apply for the low-lying resonance state with an extremely narrow width. Further, difficulties can arise in obtaining the values of δ_ℓ from the computed S matrix, $S_\ell = e^{2i\delta_\ell}$ or $\tan\delta_\ell$. On the other hand, one can directly find the value of resonance energy and the width from the pole of S_ℓ in the complex energy plane. In our recent publication [25], having located these resonant poles, we have calculated results of decay time of α emission from several nuclei and successfully explained the respective experimental data. However, we find that it is difficult to derive an analytic expression for the decay width or the half-life from the complex expression of the S matrix by any judicious approximation of the functions defining the matrix.

In the picture of transition from quasibound state to scattering state, one can express the width in terms of wave function at resonance and Coulomb functions in two ways:

(i) The normalized regular solution $u(r)$ of the modified Schrödinger equation is matched at a large distance $r = R$ to the distorted outgoing Coulomb function directly as

$$u(R) = N_0|G_0(\eta,kR) + i\,F_0(\eta,kR)|,$$

where F_0 and G_0 are the regular and irregular Coulomb functions, and the decay width is expressed [26] as

$$\Gamma = \frac{\hbar^2 k}{\mu}|N_0|. \quad (1)$$

(ii) The general formula of the α-decay width can be expressed [27] as

$$\Gamma = 2\pi|\langle\psi|H - H_0|\phi\rangle|^2, \quad (2)$$

where ψ is a bound initial state for the decaying nucleus, and ϕ is a final scattering state for the α + daughter system. The Hamiltonians H_0 and H are associated with ϕ and ψ, respectively.

Both the methods or expressions (1) and (2) of decay width are equivalent [26]. However, in the first expression (1), Γ depends on a radial distance R which is not specified exactly except that it is a large distance. Therefore, the calculated results, being sensitive to the value of R, become uncertain for explaining certain measured data. However, on the basis of the nature of spatial variation of the resonant wave function $u(r)$, we selected a distance for R, obtained analytic expression for the decay rate including a compact formula like the GN law, and explained the experimental data successfully in our recent works [28,29].

The second formula (2) of width Γ has been used by Ni and Ren [30] successfully for the estimate of α-decay rate by taking care of the dependence of the result on the value of the matching radius R. We, in this work, wish to use this expression (2) for the decay width and derive an analytic expression for half-life in terms of the resonant wave function of an exactly solvable potential and the regular Coulomb function. Further, by using some judicious approximations for the functions in the above expression of half-life, we derive a compact formula for the logarithm of half-life in terms of only the decay energy and mass and charge numbers of the α emitter. This well-defined formula resembles the form of the empirical VS rule [18,19] of α-decay rate. The application of the expression of half-life or the compact formula of logarithm of half-life to the analysis of measured data of half-life of variety of nuclei with extremely large as well as very small decay half-lives gives us remarkable success in explaining the respective experimental data. In particular, the plot of our results of logarithm of half-lives as a function of the quantity similar to the VS parameter gives us a perfect straight line and explains the corresponding linear alignment of the experimental results very well.

Further, having known the Q_α value from the atomic mass tables at a given state of emission and the mass, A_D, and charge, Z_D, numbers of the daughter nucleus, our closed formula can predict the results of α-decay half-life for all types of α-emitting nuclei: even-odd, odd-even, or odd-odd nuclei with the specified ℓ values. The available results of experimental values of α-decay half-lives with $\ell = 0$ as well as $\ell > 0$ for several nuclei could be explained closely by the predicted results. We also record the predicted values of decay rates for large number of nuclei for which measured results of α-decay rate are not known. These results would be useful for future experiments and identification.

In Sec. II, the details of the formulation and derivation of the expressions for decay half-lives and the closed formula for logarithm of half-lives are given. Section III discusses the applications of the formulation to the explanation of the experimental data. In Sec. IV, we record the conclusion of the work.

II. THE THEORETICAL FRAMEWORK

A. Decay width or half-life of α decay

Within the concept of decay as the transition of an α cluster from an isolated quasibound state to a scattering state, the decay width is a resonance width in the potential scattering process with α cluster as the projectile and the residual daughter nucleus as the target. The decay width is expressed generally by (2), which can be presented in the form (6) below, as done in Ref. [30]. The final-state wave function describing the motion of the α particle relative to the daughter nucleus can be written as a scattering state wave function corresponding to the α particle in the point-charge Coulomb potential. Its radial part is [31]

$$\phi_\ell(r) = \sqrt{\frac{2\mu}{\pi\hbar^2 k}}\frac{F_\ell}{r}, \tag{3}$$

where $k = \sqrt{2\mu E_{\text{c.m.}}}/\hbar$, $E_{\text{c.m.}}$ stands for the center-of-mass energy, $\mu = m_n \frac{A_\alpha A_D}{A_\alpha + A_D}$ represents the reduced mass of the system with m_n giving the mass of a nucleon, and F_ℓ is the regular Coulomb wave function for a given partial wave ℓ. The factor $\sqrt{\frac{2\mu}{\pi\hbar^2 k}}$ is a normalization factor of the scattering wave function. The initial-state wave function describes the quasibound state of α cluster in the decaying nucleus. Its radial wave function,

$$\psi_{n\ell}(r) = \frac{u_{n\ell}}{r}, \tag{4}$$

is achieved through exact solution of the Schrödinger equation with an effective potential, which is a combination of nuclear potential and the electrostatic potential. The details of this course will be presented in the next section.

The α cluster in the decaying nucleus is governed by an attractive nuclear potential, $V_N(r)$, and a repulsive Coulomb potential of a homogeneously charged sphere in the region close to the origin, while the α particle away from the origin experiences the sole point-charge Coulomb potential $V_c^p(r) = Z_\alpha Z_D e^2/r$, where $e^2 = 1.4398$ MeV fm. $H - H_0$ is considered as the difference between the potentials in the two situations, that is,

$$H - H_0 = \{V_N(r) + V_c(r)\} - V_c^p(r) = V_{\text{eff}}(r) - V_c^p(r). \tag{5}$$

Through the application of mean-field approximation [32] for the nucleon-nucleon interaction and the process of double folding the α + nucleus potential $V_N(r)$ with the electrostatic term in parabolic form is obtained at close radial distances r. This combined potential $V_{\text{eff}}(r)$ is very closely simulated by an expression as a function of distance and is solved exactly in the Schrödinger equation [28]. Considering this solution as the wave function $u_{n\ell}(r)$ for $\ell = 0$ in the interior region, the expression (2) of the decay width reduces to

$$\Gamma = \frac{4\mu}{\hbar^2 k}\frac{|\int_0^R F_\ell[V_{\text{eff}}(r) - V_c^p(r)]u_{n\ell}(r)dr|^2}{\int_0^R |u_{n\ell}(r)|^2 dr}. \tag{6}$$

This formulation [33,34] for Γ is based on a Gell-Mann-Goldberger transformation [26] and is used in Ref. [26] for the study of proton-decay life times. The factor $\int_0^R |u_{n\ell}(r)|^2 dr$ is used for the normalization of the interior wave function $u_{n\ell}(r)$. Since the resonant wave function $u_{n\ell}(r)$ decreases rapidly with distance outside the Coulomb barrier radius (r_B) it can be normalized (box normalization) by requiring that $\int_0^R |u_{n\ell}(r)|^2 dr = 1$, where $R \approx r_B$. Then the α-decay half-life is related to the decay width by the well-known relationship $T_{1/2} = \hbar ln2/\Gamma$. Using Γ given by (6), $T_{1/2}$ is expressed as

$$T_{1/2} = \frac{0.693\hbar^3 k}{4\mu}\frac{1}{J}, \tag{7}$$

$$J = \left|\int_0^R F_\ell[V_{\text{eff}}(r) - V_c^p(r)]u_{n\ell}(r)dr\right|^2. \tag{8}$$

Using the Sommerfeld parameter $\eta = \frac{\mu}{\hbar^2}\frac{Z_\alpha Z_D e^2}{k}$, we can express the regular Coulomb wave function $F_\ell(r)$ as follows [35]:

$$F_\ell(r) = A_\ell \rho^{\ell+1} f_\ell(\rho), \tag{9}$$

where $\rho = kr$,

$$f_\ell(\rho) = \int_0^\infty (1 - \tanh^2\epsilon)^{\ell+1}\cos(\rho\tanh\epsilon - 2\eta\epsilon)d\epsilon, \tag{10}$$

$$A_\ell = \frac{\sqrt{1 - \exp(-2\pi\eta)}}{2^\ell\{2\pi\eta(1+\eta^2)(2^2+\eta^2)\dots(\ell^2+\eta^2)\}^{\frac{1}{2}}}. \tag{11}$$

In particular, for $\ell = 0$, A_ℓ is given by

$$A_0 = \left\{\frac{1 - \exp(-2\pi\eta)}{2\pi\eta}\right\}^{\frac{1}{2}}. \tag{12}$$

For a typical case of α + daughter (α + ^{174}Hg) system with energy $E = 7.79$ MeV, usually called the Q value of decay, Figs. 1(a)–1(d) illustrate the radial dependence of the three terms in the integrand $J_1 = |\int_0^R F_\ell[V_{\text{eff}}(r) - V_c^p(r)]u_{n\ell}(r)dr|$ of Eq. (8): the modulus of the resonance state wave function, $|u(r)|$, at resonance energy $E = 7.79$ MeV, the regular Coulomb wave function, $F_0(r)$, for $\ell = 0$, and the combined nuclear and Coulomb potential, $V_{\text{eff}}(r)$ (upper panel) that generates the resonance energy 7.79 MeV and the difference in potentials, $V_{\text{eff}}(r) - V_c^p(r)$ (lower panel). The total integrand J_1 multiplied by a scaling factor 10^{11} is shown in Fig. 1(d). As clearly seen, the integrand shows a peak in the region close to the Coulomb barrier radius, $r_B = 9.2$ fm. This is because the Coulomb function is vanishingly small at small r values, while the wave function of the resonant state decreases exponentially in the barrier region along with the value of the potential difference ($V_{\text{eff}} - V_c^p$) becoming zero in the region $r \geqslant r_B$. The α-decay rate is thus expected to depend rather weakly on the detailed structure of the wave function in the interior part of the nucleus, while the contribution to it from the region $r \geqslant r_B$ is negligibly small. As a result of this, though the integrand in expression (8) for the quantity J shows explicit dependence on distance $r = R$ as the upper limits of integration, the value of J does not change much due to some change in the value of R in the region beyond r_B. Hence, the value of decay time $T_{1/2}$ [Eq. (7)], depending on the result of J, remains practically independent of the choice of the distance R in region $r \geqslant r_B$.

B. The effective α + nucleus potential and exact solution

The potential which simulates the total effective potential of a typical α + nucleus system is expressed analytically as a

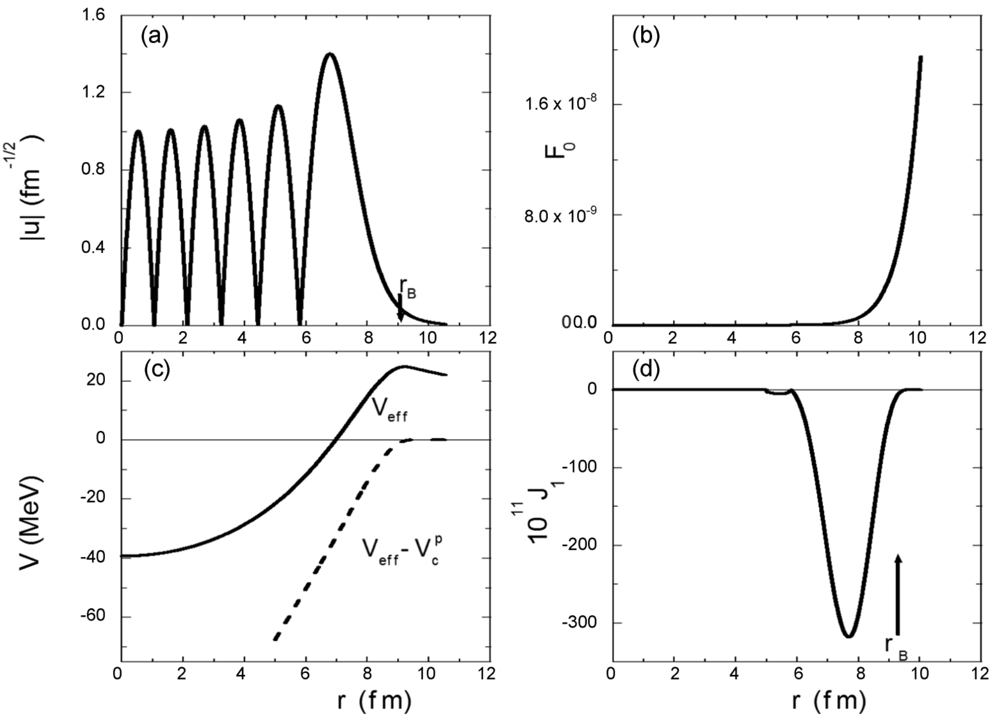

FIG. 1. Different terms contributing to the α-decay rate in s-wave state in the ^{178}Pb parent nucleus: (a) the modulus of the radial wave function at resonance, (b) the regular Coulomb wave function, and (c) the α + daughter potential, $V_{\rm eff}$, in upper panel and the potential difference, $V_{\rm eff} - V_c^p$, in lower panel. In panel (d) the integral $J_1 = |\int_0^R F_\ell(V_{\rm eff}(r) - V_c^p(r))u_{n\ell}(r)dr|$ multiplied by 10^{11} is shown in the case of the s wave. The barrier radius at $r_B = 9.2$ fm is indicated by arrows.

function of radial distance r as follows [28]:

$$V_{\rm eff}(r) = \begin{cases} V_{01}\{\lambda_1^2[B_0 + (B_1 - B_0)(1 - y_1^2)] + \xi_1\} & \text{if} \quad 0 < r < R_1 \\ V_{02}\{\lambda_2^2 B_2(1 - y_2^2) + \xi_2\} & \text{if} \quad r \geqslant R_1, \end{cases} \tag{13}$$

where

$$\xi_1 = \left(\frac{1-\lambda_1^2}{4}\right)[5(1-\lambda_1^2)y_1^4 - (7-\lambda_1^2)y_1^2 + 2](1-y_1^2),$$

$$\xi_2 = \left(\frac{1-\lambda_2^2}{4}\right)[5(1-\lambda_2^2)y_2^4 - (7-\lambda_2^2)y_2^2 + 2](1-y_2^2).$$

Here, V_{01} and V_{02} are the strengths of the potential in MeV. Denoting the mass of the particle moving under the potential by μ, we use dimensionless variable $\rho_n = (r - R_1)b_n$ with $b_n = (\frac{2m}{\hbar^2}V_{0n})^{1/2}$, $n = 1,2$, such that ρ_n is related to the new variable y_n as $\rho_n = \frac{1}{\lambda_n^2}[\tanh^{-1} y_n - (1-\lambda_n^2)^{1/2}\tanh^{-1}(1-\lambda_n^2)^{1/2}y_n]$.

The parameters λ_1, B_0, and B_1 specify the potential in the interior region $r < R_1$ and the parameters λ_2 and B_2 specify the potential in the outer region $r > R_1$. The expression (13) generates a potential barrier at $r = R_1$ or $y_1 = y_2 = 0$ with the height V_B of the barrier expressed as $V_B = V_{01}[\lambda_1^2 B_1 + \frac{1-\lambda_1^2}{2}]$, so that $V_{01} = V_B/[\lambda_1^2 B_1 + \frac{1-\lambda_1^2}{2}]$.

One can use the global expressions for the radial position $R_1 = r_B = r_0(A_\alpha^{1/3} + A_D^{1/3}) + 2.72$, and the height $V_B = \frac{Z_\alpha Z_D e^2}{R_1}(1 - \frac{a_0}{R_1})$ for the barrier potential, where r_0 and a_0 are two distance parameters expressed in femtometers. The values of r_B and V_B obtained through these expressions for an α + nucleus system are consistent with properties of combined Coulomb-nuclear potential found suitable for the description of scattering event of the system.

Using the potential given above, the Schrödinger equation is solved for the wave function, which is expressed as a function of r. The solution $u_1(\rho_1)$ in the region $r \leqslant R_1$ can be obtained from Ref. [28].

The potential, having a pocket followed by a repulsive barrier, can generate eigenstates with discrete positive energies, which are known as resonance states. Exactly at the resonance energy, the wave function looks like a bound-state wave function depicting the confinement property that the probability amplitude $\mathrm{I} = \int |u_1(r)|^2 dr$ in the interior region $0 < r < R_1$ is very large as compared to that in the outer region $(r > R_1)$. Selecting two distances R_1 and R_2 with $R_2 > R_1$, the ratio of the probability amplitudes

$$P = \frac{\int_0^{R_1} |u_1(r)|^2 dr}{\int_0^{R_2} |u_1(r)|^2 dr} \tag{14}$$

is calculated at a given incident energy $E_{\rm c.m.}$. In the variation of the quantity P with energy, the value of the energy for which $P \approx 1$ gives the resonance energy or Q_α energy of the decaying α particle.

The α + nucleus potential, which can be obtained by calculations based on mean-field theoretic approaches [32], is closely reproduced by our analytically solvable potential [Eq. (13)] by fixing the values of the parameters, namely $r_0, a_0, B_0, b_1 = \sqrt{B_1}A_D^{-1/3}$, and λ_1. It is obvious that different parent nuclei decaying through α-decay mode with the characteristic Q_α value would experience different interaction potentials for their corresponding α + daughter systems depending on the values of mass number A and atomic number Z of the nucleus. Keeping the values of four parameters fixed at $r_0 = 0.97$ fm, $a_0 = 1.6$ fm, $\lambda_1 = 1.6$, and $\sqrt{B_1} = 6.2$, the variation in the potential is achieved by changing the value of the remaining one parameter, namely B_0, that specifies the depth of the effective potential. In other words, at the incident energy $E_{\mathrm{c.m.}} = Q_\alpha$ of α+daughter system, the quantity P (14) is varied as a function of B_0. The value of B_0 for which $P \approx 1$ becomes the optimum value for the depth of the potential which would generate resonance (quasi-bound) state at the energy that is equal to Q_α.

C. Closed form expression for logarithm of decay half-life

For a typical α + nucleus system with its characteristic Q_α energy value and radius $R = r_B$, the values of Sommerfeld parameter η and parameter $\rho = kR$ are such that the product $\eta\rho \leqslant 50$ and $\rho \approx 10$. In this situation, one can express the regular Coulomb wave function $F_\ell(r)$ by using power series expansion [35] and write

$$F_\ell^{ps}(r) = C_\ell \rho^{\ell+1} G_\ell, \tag{15}$$

$$(n+1)(n+2\ell+2)G_{n+1} = 2\eta\rho G_n - \rho^2 G_{n-1}, \tag{16}$$

$$\mathrm{G}_0 = 1, \quad \mathrm{G}_1 = \frac{\eta\rho}{(\ell+1)},$$

$$\mathrm{G}_\ell = \sum_j G_j,$$

$$C_\ell^2 = \frac{P_\ell(\eta)}{2\eta}\frac{C_0^2(\eta)}{(2\ell+1)}, \tag{17}$$

$$P_\ell(\eta) = \frac{2\eta(1+\eta^2)(4+\eta^2)\dots(\ell^2+\eta^2)2^{2\ell}}{(2\ell+1)[(2l)!]^2}. \tag{18}$$

In particular, for $\ell = 0$, $P_0(\eta) = 2\eta$, and

$$C_0^2(\eta) = 2\pi\eta\{\exp(2\pi\eta) - 1\}^{-1}, \tag{19}$$

$$F_0^{ps}(r) = C_0\rho G_0, \tag{20}$$

where G_0 is equal to G_ℓ derived through expression (16) taking $G_1 = \eta\rho$ for $\ell = 0$.

In Fig. 2, we compare the results of $F_\ell^{ps}(r)$ as a function of r with the accurate values of $F_\ell(r)$ given by expression (9) for $\ell = 0$ and find that

$$F_\ell(r) = x_m F_\ell^{ps}(r), \tag{21}$$

with $x_m \approx 70$. Thus, the computation of the function $F_\ell(r)$ through expression (9) could be avoided by using a simple expression (15) multiplied by a factor $x_m = 70$. The variation of $F_\ell(r) = x_m F_\ell^{ps}(r)$ with radial distance r as shown in Fig. 2

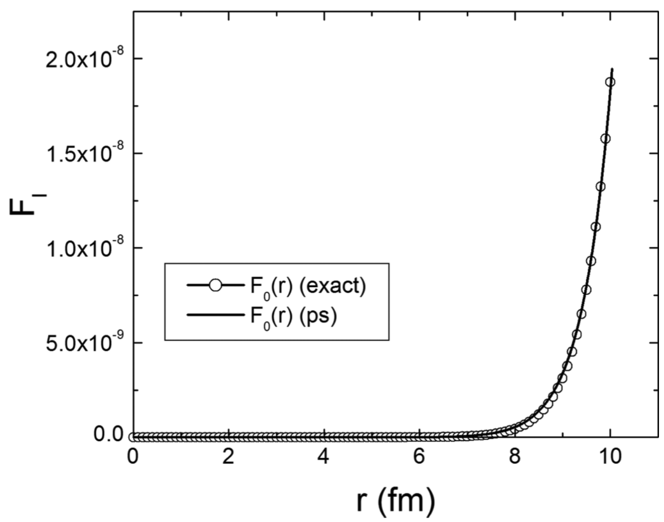

FIG. 2. Comparison of spatial variation of exact regular Coulomb wave function $F_0(r)$ (exact) given by Eq. (9) with the results $F_0(r)(ps) = x_m F_0^{ps}(r)$, $x_m = 70$, given in terms of power series expansion function $F_\ell^{ps}(r)$ of (15) for $\ell = 0$ in a typical case of $\alpha + {}^{174}$Hg system.

indicates that the magnitude of this function is zero near the origin $r = 0$ and it increases sharply at a distance around the the Coulomb barrier position $r = r_B$. Further, the resonant wave function $u_{n\ell}(r)$ attains negligibly small values in the region beyond $r = r_B$. In view of this, the integral J given by expression (8) can be equated to the value of $F_\ell(r) = x_m F_\ell^{ps}(r)$ at a point $r = R = r_B$ with some multiplying factor to account for the contributions to the integral from other regions within $0 < r < R$ such that

$$J = |c_f F_\ell(R)|^2 = \left|c_f x_m F_\ell^{ps}(R)\right|^2. \tag{22}$$

The value of $c_f (= \sqrt{J}/|x_m F_\ell^{ps}(R)|)$ for a typical α + nucleus system is found to be of the order of 0.22 in the case of $\ell = 0$.

Using the simplified result for J given by (22) in terms of $F_\ell^{ps}(R)$ expressed by (15) with $C_0^2(\eta) \approx \frac{2\pi\eta}{\exp(2\pi\eta)}$ due to large value of $2\pi\eta$, the expression (7) for decay half-life $T_{1/2}$ reduces to

$$T_{1/2} = 0.693\hbar q_\ell \frac{\exp(2\pi\eta)}{f_{m\ell}^2}, \tag{23}$$

where

$$q_\ell = \frac{2\eta(2\ell+1)}{P_\ell(\eta)\rho^{2\ell}}, \tag{24}$$

$$f_{m\ell} = \sqrt{4\mu/\hbar^2 k}\sqrt{2\pi\eta}c_f x_m \rho G_\ell. \tag{25}$$

Taking the logarithm of both sides, we get

$$\log T_{1/2} = a\chi + c + d + b_\ell, \tag{26}$$

$$a = 1.4398\pi\sqrt{2(931.5)}/197.329, \tag{27}$$

$$\chi = Z_\alpha Z_D \sqrt{\frac{A_\alpha A_D}{(A_\alpha + A_D)Q_\alpha}}, \tag{28}$$

$$c = -2\log S, \tag{29}$$

$$d = -2\log D, \tag{30}$$

$$b_\ell = \log(q_\ell), \tag{31}$$

$$S = c_f x_m R G_\ell\left(\frac{A_\alpha A_D\sqrt{Z_\alpha Z_D}}{A_\alpha + A_D}\right), \tag{32}$$

$$D = \frac{2 \times 931.5 \times \sqrt{1.4398 \times 2\pi}}{(197.329)^2\sqrt{0.693 \times 197.329 \times 0.333 \times 10^{-23}}}. \tag{33}$$

The formula (26) is found to be similar to the VS relation [18,19], $\log_{10}T_{1/2} = \frac{a'Z_D+b'}{\sqrt{Q_\alpha}} + c'Z_D + d'$, where $a' = 1.478$, $b' = 8.714$, $c' = -0.183$, and $d' = -34.699$. But, unlike the VS formula all the parameters and coefficients, a, c, d, and b_ℓ in our expression (26) are well defined. Here, the coefficient $a = 2.693$ and the constant $d = -45.262$. The parameter c given by (29) is not a constant but depends critically on A_D, Z_D, and Q_α values, and angular momentum partial wave (ℓ) through the factor S (32). Further, the formula (26) contains an extra parameter $b_\ell = \log(q_\ell)$ which depends on ℓ along with the Q value through the expression (24) for q_ℓ to account for the decay time of α particle emitting with some angular momenta ℓ. The plot of the results of $\log T_{1/2}$ as a function of the quantity $V = a\chi + c$ in (26) with $\ell = 0$, similar to the VS parameter $\tilde{V} = \frac{a'Z_D+b'}{\sqrt{Q_\alpha}} + c'Z_D$, shows a perfect linear path to explain the rectilinear variation of the experimental data as a function of the same quantity $V = a\chi + c$. This will be demonstrated in the next section while explaining the measured results of α-decay half-lives.

III. NUMERICAL RESULTS AND DISCUSSION

We use the solvable potential given by expression (13) for the effective Coulomb-nuclear potential for the α + nucleus system and vary the depth of the potential to reproduce the result of α-decay energy Q_α of any nucleus as a resonance energy. Then, using the same resonance energy Q_α and the spatial variation of exact wave function $u_{n\ell}(r)$ at resonance, the result of half-life $T_{1/2}$ of α decay is calculated by computing the expression (7). This calculated value of $T_{1/2}$ denoted by $T_{1/2}^{(\mathrm{calt})}$ is then compared with the experimental result of $T_{1/2}$ denoted by $T_{1/2}^{(\mathrm{expt})}$ for its explanation. Thus, in this analysis, we do not fit the experimental value of half-life; rather, we explain it by the result of $T_{1/2}^{(\mathrm{calt})}$ calculated independently from the quantal theory of decay in the resonance state at energy Q_α of the system.

In Table I, we present the measured results of Q_α values denoted by $Q_\alpha^{(\mathrm{expt})}$, the corresponding results of half-lives from experiment $T_{1/2}^{(\mathrm{expt})}$ [36], and the results of present calculation $T_{1/2}^{(\mathrm{calt})}$ using the expression (7) for several isotopes of Pb element with $A = 178$–208. Starting from the small value $T_{1/2}^{(\mathrm{expt})} = 1.2 \times 10^{-4}$ s for low-mass isotope ^{178}Pb to large time $T_{1/2}^{(\mathrm{expt})} = 8.8 \times 10^{9}$ s for the case of ^{194}Pb, almost all the experimental values are explained quite well by our calculated results, presented in the fourth column as $T_{1/2}^{(\mathrm{calt})}$.

In the process of the computation of the integral J given by expression (8), we estimate the value of the parameter c_f

TABLE I. Comparison of experimental results of α-decay half-life $T_{1/2}^{(\mathrm{expt})}$ with the calculated results $T_{1/2}^{(\mathrm{calt})}$ obtained by using formula (7) and predicted values $T_{1/2}^{(\mathrm{pred})}$ derived from $\log_{10}T_{1/2}^{(\mathrm{pred})}$ given by formula (26). Experimental data of α-decay half-life and $Q_\alpha^{(\mathrm{expt})}$ are obtained from Ref. [36].

Decay	$Q_\alpha^{(\mathrm{expt})}$ (MeV)	$T_{1/2}^{(\mathrm{expt})}$ (s)	$T_{1/2}^{(\mathrm{calt})}$ (s)	$T_{1/2}^{(\mathrm{pred})}$ (s)
^{178}Pb → ^{174}Hg	7.790	1.2×10^{-4}	2.46×10^{-4}	3.29×10^{-4}
^{180}Pb → ^{176}Hg	7.419	4.2×10^{-3}	3.32×10^{-3}	3.96×10^{-3}
^{182}Pb → ^{178}Hg	7.066	5.61×10^{-2}	4.79×10^{-2}	5.08×10^{-2}
^{184}Pb → ^{180}Hg	6.774	6.13×10^{-1}	5.06×10^{-1}	4.92×10^{-1}
^{186}Pb → ^{182}Hg	6.470	1.21×10^{1}	7.33×10^{0}	6.28×10^{0}
^{188}Pb → ^{184}Hg	6.109	2.70×10^{2}	2.17×10^{2}	1.70×10^{2}
^{190}Pb → ^{186}Hg	5.697	1.72×10^{4}	1.67×10^{4}	1.12×10^{4}
^{192}Pb → ^{188}Hg	5.221	3.56×10^{6}	4.85×10^{6}	2.76×10^{6}
^{194}Pb → ^{190}Hg	4.738	8.8×10^{9}	3.62×10^{9}	1.78×10^{9}
^{196}Pb → ^{192}Hg	4.226		1.36×10^{13}	0.58×10^{13}
^{198}Pb → ^{194}Hg	3.709		3.20×10^{17}	1.18×10^{17}
^{200}Pb → ^{196}Hg	3.151		3.25×10^{23}	0.80×10^{23}
^{202}Pb → ^{198}Hg	2.590			4.28×10^{30}
^{204}Pb → ^{200}Hg	1.969			7.48×10^{42}
^{206}Pb → ^{202}Hg	1.135			2.55×10^{73}
^{208}Pb → ^{204}Hg	0.5172			5.73×10^{134}

used in Eq. (22) to represent the total contributions of the integral J in terms of the Coulomb function at a fixed distance $r = R = r_B$ for different nuclei in the series of isotopes and find that the values of c_f are within the narrow range 0.2–0.26 in the case of $\ell = 0$. We use $c_f = 0.22$ for all Pb isotopes and estimate the values of $T_{1/2}$ by using the closed form expression (26) for the decimal logarithm of half-life $\log_{10}T_{1/2}^{(\mathrm{pred})} = \log T_{1/2}^{(\mathrm{pred})}/2.30258$. We extract the values of $T_{1/2}^{(\mathrm{pred})}$ from the above results of $\log_{10}T_{1/2}^{(\mathrm{pred})}$ and present them in the fifth column of Table I. As we have approximated the integral J by the function $F_\ell^{ps}(R)$ at a single point $r = R = r_B$, we call this results of $T_{1/2}$ predicted or approximate results denoted as $T_{1/2}^{(\mathrm{pred})}$. As we see clearly in this table, the predicted results, $T_{1/2}^{(\mathrm{pred})}$, are very close to the respective values of $T_{1/2}^{(\mathrm{calt})}$ calculated using the formula (7) with direct computation of the integral J given by (8).

We compare our precisely calculated results, $T_{1/2}^{(\mathrm{calt})}$, in the form of decimal logarithm $\log_{10}T_{1/2}^{(\mathrm{calt})}$ as a function of Q_α with those from experiments ($\log_{10}T_{1/2}^{(\mathrm{expt})}$) in Fig. 3. As seen clearly, the available measured results denoted by solid dots are explained nicely by our results, $\log_{10}T_{1/2}^{(\mathrm{calt})}$, represented by a solid curve. The results of $\log_{10}T_{1/2}^{(\mathrm{pred})}$ calculated by using the closed form expression (26) for all isotopes possessing large as well as very small Q_α values are presented as a dashed curve in the same Fig. 3. We see that these predicted results explain the available experimental data (solid dots) as satisfactorily as the results $\log_{10}T_{1/2}^{(\mathrm{calt})}$ shown by a solid curve. Further, the same dashed curve in continuation shows the very large values of $\log_{10}T_{1/2}^{(\mathrm{pred})}$ for heavy isotopes with small Q_α values. We believe that these results will guide the

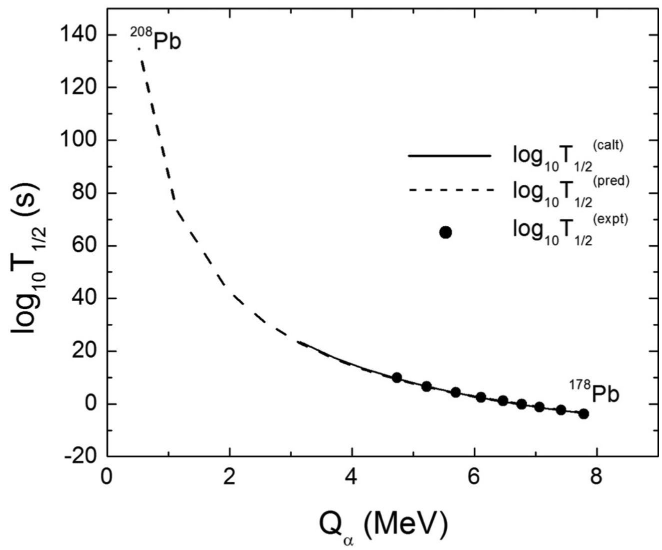

FIG. 3. The logarithm of α-decay half-lives for different isotopes of Pb nucleus. The solid curve represents calculated results $\log_{10} T_{1/2}^{(\mathrm{calt})}$ using formula (7) and the dashed curve represents the predicted values $\log_{10} T_{1/2}^{(\mathrm{pred})}$ calculated using formula (26) with $\ell = 0$. Experimental results $\log_{10} T_{1/2}^{(\mathrm{expt})}$ shown by solid dots are obtained from Table I of Ref. [36].

experimentalists while trying to measure the decay half-lives of these neutron-enriched nuclei possessing small Q_α values.

We now consider a set of even-even nuclei for which experimental data of Q_α and α decay half-lives for ground-state to ground-state transition with $\ell = 0$ are available. In Table II, the first column denotes the parent α-decaying nucleus, the second column represents the α-decay energy Q_α of the nucleus derived from the nuclear mass table by Audi *et al.* [37,38], and the third column contains the logarithm of experimental half-life, $\tau^{(\mathrm{expt})} = \log_{10} T_{1/2}^{(\mathrm{expt})}$, obtained from Refs. [39,40]. In the fourth column we present the logarithm of $T_{1/2}^{(\mathrm{calt})}$, $\tau^{(\mathrm{calt})} = \log_{10} T_{1/2}^{(\mathrm{calt})}$, obtained by computing expression (7). In the fifth column, we record the results of logarithm of $T_{1/2}$ calculated by using the closed-form expression (26) denoted by $\tau^{(\mathrm{pred})} = \log_{10} T_{1/2}^{(\mathrm{pred})}$ where we have used $c_f = 0.22$ for all nuclei. As we see in the fourth and fifth columns of the table, the results of $\log_{10} T_{1/2}^{(\mathrm{calt})}$ and $\log_{10} T_{1/2}^{(\mathrm{pred})}$ are very close with each other and they explain the corresponding experimental values, $\log_{10} T_{1/2}^{(\mathrm{expt})}$, reported in third column for 136 cases of even-even nuclei with remarkable success. We now wish to compare these calculated results with the corresponding experimental values in graphical forms.

In Fig. 4, the results of $\log_{10} T_{1/2}^{(\mathrm{expt})}$ and $\log_{10} T_{1/2}^{(\mathrm{pred})}$ are plotted as a function of the Coulomb parameter $\chi = Z_\alpha Z_D \sqrt{\frac{A_\alpha A_D}{(A_\alpha + A_D) Q_\alpha}}$ as done in Geiger-Nuttall law. It is seen that the experimental data (solid dots) do not fall in a narrow linear path but they are scattered. Our calculated results of $\log_{10} T_{1/2}^{(\mathrm{pred})}$ are shown by solid lines. It is seen that instead of a single straight line there are many linear lines almost parallel to each other in this presentation and they are found to cover the corresponding measured data (solid dots) in close proximity. However, the comparison of the results in this form of plotting

TABLE II. Comparison of experimental results of ground-state to ground-state ($\ell = 0$) α-decay half-life $\tau^{(\mathrm{expt})} = \log_{10} T_{1/2}^{(\mathrm{expt})}$ in seconds with the calculated results $\tau^{(\mathrm{calt})} = \log_{10} T_{1/2}^{(\mathrm{calt})}$ in seconds obtained by using formula (7) and predicted values $\tau^{(\mathrm{pred})} = \log_{10} T_{1/2}^{(\mathrm{pred})}$ in seconds given by formula (26). Experimental data of α-decay half-life and Q_α value in MeV are obtained from Refs. [37–40].

${}^{A}_{Z}$	Q_α	$\tau^{(\mathrm{expt})}$	$\tau^{(\mathrm{calt})}$	$\tau^{(\mathrm{pred})}$
${}^{106}_{52}$	4.290	−4.15	−4.12	−3.93
${}^{108}_{52}$	3.445	0.49	0.47	0.52
${}^{112}_{54}$	3.33	2.53	2.59	2.55
${}^{114}_{56}$	3.53	1.77	2.56	2.49
${}^{144}_{60}$	1.905	22.86	23.21	23.15
${}^{146}_{62}$	2.528	15.51	15.66	15.54
${}^{148}_{62}$	1.986	23.34	23.74	23.57
${}^{148}_{64}$	3.271	9.37	9.44	9.38
${}^{150}_{64}$	2.808	13.75	13.97	13.84
${}^{152}_{64}$	2.203	21.53	21.98	21.74
${}^{150}_{66}$	4.351	3.08	3.03	3.07
${}^{152}_{66}$	3.726	6.93	7.12	7.07
${}^{154}_{66}$	2.946	13.98	14.00	13.84
${}^{152}_{68}$	4.934	1.06	1.01	1.08
${}^{154}_{68}$	4.28	4.68	4.62	4.59
${}^{154}_{70}$	5.474	−0.35	−0.46	−0.36
${}^{156}_{70}$	4.811	2.42	2.71	2.71
${}^{158}_{70}$	4.172	6.63	6.48	6.40
${}^{156}_{72}$	6.028	−1.63	−1.77	−1.64
${}^{158}_{72}$	5.405	0.81	0.83	0.87
${}^{160}_{72}$	4.902	3.29	3.29	3.27
${}^{162}_{72}$	4.417	5.69	6.08	5.98
${}^{174}_{72}$	2.497	22.8	23.85	23.98
${}^{160}_{74}$	6.065	−0.99	−1.00	−0.92
${}^{162}_{74}$	5.677	0.48	0.58	0.61
${}^{164}_{74}$	5.278	2.22	2.41	2.38
${}^{166}_{74}$	4.856	4.74	4.60	4.51
${}^{180}_{74}$	2.508	25.75	25.68	25.43
${}^{162}_{76}$	6.767	−2.73	−2.69	−2.55
${}^{166}_{76}$	6.139	−0.52	−0.41	−0.36
${}^{168}_{76}$	5.818	0.62	0.90	0.90
${}^{170}_{76}$	5.539	1.79	2.13	2.09
${}^{172}_{76}$	5.227	3.98	3.64	3.55
${}^{174}_{76}$	4.872	5.34	5.54	5.40
${}^{186}_{76}$	2.823	22.8	22.73	22.57
${}^{168}_{78}$	6.997	−2.7	−2.66	−2.54
${}^{170}_{78}$	6.708	−1.85	−1.68	−1.61
${}^{174}_{78}$	6.184	0.03	0.26	0.26
${}^{176}_{78}$	5.885	1.22	1.50	1.46
${}^{178}_{78}$	5.573	2.45	2.91	2.82
${}^{180}_{78}$	5.24	4.24	4.55	4.41
${}^{188}_{78}$	4.008	12.53	12.10	12.07
${}^{190}_{78}$	3.251	19.31	19.09	18.97
${}^{174}_{80}$	7.233	−2.7	−2.65	−2.55
${}^{176}_{80}$	6.897	−1.69	−1.53	−1.48
${}^{180}_{80}$	6.258	0.73	0.84	0.80
${}^{182}_{80}$	5.997	1.86	1.92	1.85
${}^{184}_{80}$	5.662	3.44	3.44	3.31

TABLE II. (*Continued.*)

$^{A}_{Z}$	Q_α	$\tau^{(\mathrm{expt})}$	$\tau^{(\mathrm{calt})}$	$\tau^{(\mathrm{pred})}$
$^{186}_{80}$	5.205	5.71	5.74	5.56
$^{188}_{80}$	4.705	8.72	8.67	8.41
$^{186}_{82}$	6.47	0.68	0.59	0.79
$^{188}_{82}$	6.109	2.06	2.07	2.23
$^{190}_{82}$	5.697	4.25	3.94	4.05
$^{192}_{82}$	5.221	6.57	6.39	6.44
$^{194}_{82}$	4.738	9.99	9.26	9.25
$^{210}_{82}$	3.792	16.57	16.06	16.15
$^{190}_{84}$	7.693	−2.59	−2.89	−2.58
$^{192}_{84}$	7.319	−1.48	−1.70	−1.44
$^{194}_{84}$	6.987	−0.38	−0.57	−0.34
$^{196}_{84}$	6.657	0.77	0.65	0.83
$^{198}_{84}$	6.309	2.27	2.05	2.18
$^{200}_{84}$	5.981	3.66	3.48	3.57
$^{202}_{84}$	5.701	5.13	4.80	4.85
$^{204}_{84}$	5.485	6.28	5.89	5.91
$^{206}_{84}$	5.327	7.14	6.72	6.72
$^{210}_{84}$	5.407	7.08	6.24	6.24
$^{212}_{84}$	8.954	−6.52	−6.63	−6.19
$^{214}_{84}$	7.833	−3.78	−3.60	−3.30
$^{216}_{84}$	6.906	−0.84	−0.52	−0.34
$^{218}_{84}$	6.115	2.27	2.66	2.74
$^{198}_{86}$	7.349	−1.18	−1.03	−0.80
$^{204}_{86}$	6.545	2.01	1.93	2.05
$^{206}_{86}$	6.384	2.74	2.58	2.68
$^{208}_{86}$	6.261	3.37	3.09	3.17
$^{210}_{86}$	6.159	3.95	3.52	3.59
$^{212}_{86}$	6.385	3.16	2.51	2.60
$^{214}_{86}$	9.208	−6.57	−6.55	−6.12
$^{216}_{86}$	8.200	−4.35	−3.91	−3.61
$^{218}_{86}$	7.263	−1.46	−0.96	−0.77
$^{220}_{86}$	6.405	1.75	2.33	2.41
$^{222}_{86}$	5.590	5.52	6.17	6.14
$^{206}_{88}$	7.415	−0.62	−0.50	−0.31
$^{210}_{88}$	7.152	0.57	0.39	0.54
$^{212}_{88}$	7.032	1.18	0.82	0.95
$^{214}_{88}$	7.273	0.39	−0.09	0.07
$^{216}_{88}$	9.526	−6.74	−6.63	−6.19
$^{218}_{88}$	8.546	−4.59	−4.15	−3.84
$^{220}_{88}$	7.592	−1.74	−1.26	−1.07
$^{222}_{88}$	6.679	1.59	2.09	2.17
$^{224}_{88}$	5.789	5.52	6.14	6.11
$^{226}_{88}$	4.871	10.73	11.48	11.33
$^{216}_{90}$	8.071	−1.57	−1.95	−1.72
$^{218}_{90}$	9.849	−6.96	−6.70	−6.27
$^{220}_{90}$	8.953	−5.01	−4.53	−4.21
$^{222}_{90}$	8.127	−2.69	−2.19	−1.97
$^{224}_{90}$	7.298	0.12	0.13	0.68
$^{226}_{90}$	6.45	3.39	3.51	3.96
$^{228}_{90}$	5.52	7.93	8.11	8.47
$^{230}_{90}$	4.77	12.49	12.80	13.08
$^{232}_{90}$	4.082	17.76	18.23	18.44
$^{226}_{92}$	7.701	−0.57	−0.47	0.09

TABLE II. (*Continued.*)

$^{A}_{Z}$	Q_α	$\tau^{(\mathrm{expt})}$	$\tau^{(\mathrm{calt})}$	$\tau^{(\mathrm{pred})}$
$^{228}_{92}$	6.803	2.90	2.89	3.36
$^{230}_{92}$	5.993	6.43	6.59	6.97
$^{232}_{92}$	6.716	4.13	3.66	3.66
$^{234}_{92}$	4.858	13.04	13.52	13.55
$^{236}_{92}$	4.573	15.0	15.58	15.59
$^{238}_{92}$	4.27	17.25	18.02	17.98
$^{232}_{94}$	6.716	4.13	4.13	4.55
$^{234}_{94}$	6.31	5.89	5.96	6.34
$^{236}_{94}$	5.867	8.11	8.18	8.51
$^{238}_{94}$	5.593	9.59	9.68	9.98
$^{240}_{94}$	5.256	11.45	11.70	11.96
$^{242}_{94}$	4.985	13.18	13.47	13.70
$^{244}_{94}$	4.666	15.50	15.75	15.95
$^{238}_{96}$	6.62	5.51	5.23	5.79
$^{240}_{96}$	6.398	6.52	6.24	6.78
$^{242}_{96}$	6.216	7.28	7.30	7.63
$^{244}_{96}$	5.902	8.87	8.91	9.21
$^{246}_{96}$	5.475	11.26	11.35	11.60
$^{248}_{96}$	5.162	13.16	13.32	13.54
$^{240}_{98}$	7.719	2.03	1.80	2.26
$^{246}_{98}$	6.862	4.21	5.16	5.53
$^{248}_{98}$	6.361	7.56	7.48	7.79
$^{250}_{98}$	6.128	8.69	8.64	8.93
$^{252}_{98}$	6.217	8.01	8.15	8.45
$^{254}_{98}$	5.927	9.31	9.67	9.94
$^{246}_{100}$	8.378	0.17	0.26	0.76
$^{248}_{100}$	8.002	1.66	1.52	1.98
$^{250}_{100}$	7.557	3.38	3.14	3.55
$^{252}_{100}$	7.153	5.04	4.74	5.11
$^{254}_{100}$	7.308	4.14	4.08	4.46
$^{256}_{100}$	7.027	5.14	5.24	5.58
$^{252}_{102}$	8.55	0.74	0.42	0.90
$^{254}_{102}$	8.226	1.82	1.48	1.92
$^{256}_{102}$	8.581	0.53	0.27	0.75
$^{260}_{106}$	9.92	−2.04	−2.23	−1.66
$^{266}_{106}$	8.762	2.1	1.12	1.56

is not that clear. Further, the GN law usually designed for a single line for all α emitters would certainly fail here for the fitting of the widely scattered data.

The same experimental results $\log_{10}T_{1/2}^{(\mathrm{expt})}$ (solid dots) [39,40] along with few more [18] for Z up to 118 are plotted, in Fig. 5, as a function of the quantity $V = a\chi + c$ used in Eq. (26). This quantity V, dependent on Q_α and Z_D, is equivalent to the Viola-Seaborg parameter used in the empirical relation for the logarithm of the α-decay half-life [18,19]. It is seen that the data shown by solid dots align themselves in a narrow linear path. We show our calculated results, $\log_{10}T_{1/2}^{(\mathrm{pred})}$, as a function of $V = a\chi + c$ by a solid line in the same Fig. 5. We find that the experimental results are closely seated with the perfect straight path (solid line) generated by our calculated values. This close comparison of our results with the experimental data reveals that we have

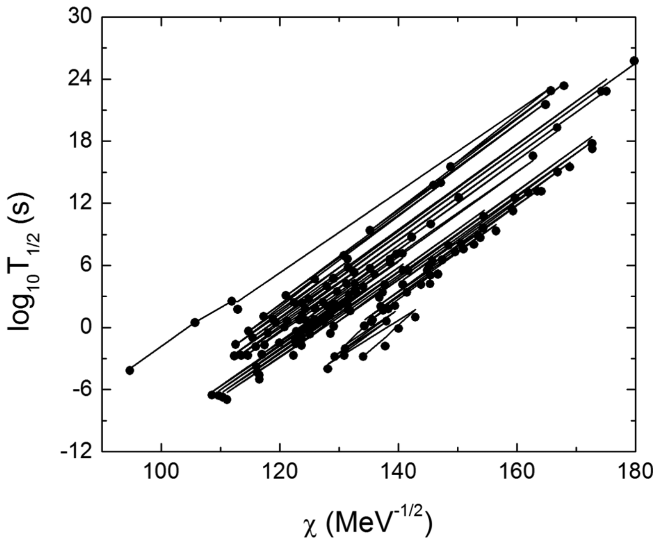

FIG. 4. Plot of decimal logarithm of half-lives $\log_{10} T_{1/2}^{(\mathrm{expt})}$ from experiments (solid dots) [39,40] and $\log_{10} T_{1/2}^{(\mathrm{pred})}$ from calculation using decay law (26) (solid line) as a function of χ in $\ell = 0$ state for α emitters with $Z = 54$–118.

been able to explain, not fit, the measured results of decay rate of α emission with remarkable success by our analytical formula (26) derived from the basic principle of decay based on the quantum theory of resonance scattering.

Besides the α decays of even-even nuclei with $\ell = 0$ state of transition analyzed above, we find in the literature plenty of experimental results of α-decay half-lives for decays of even-odd, odd-even, and odd-odd nuclei with $\ell = 0$ as well as $\ell > 0$ state of transition. Having known the Q_α value at a given state of emission from atomic mass tables or experiments and the mass, A_D, and charge, Z_D, numbers of the daughter

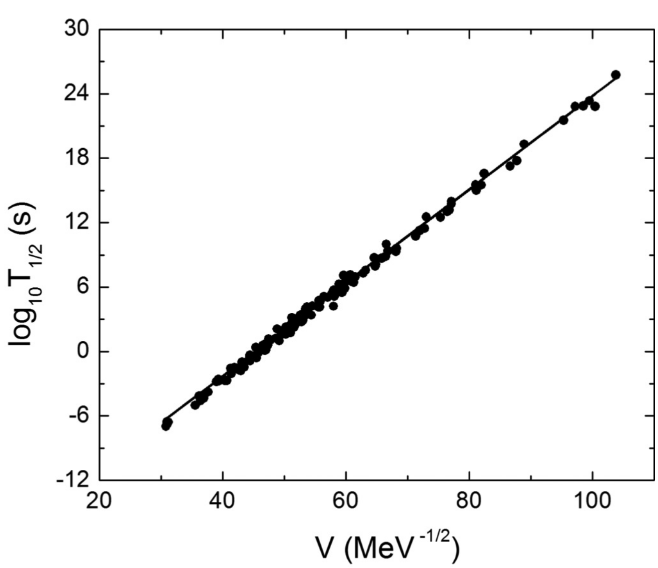

FIG. 5. Plot of decimal logarithm of half-lives $\log_{10} T_{1/2}^{(\mathrm{expt})}$ from experiments (solid dots) [18,39,40] and $\log_{10} T_{1/2}^{(\mathrm{pred})}$ from calculation using decay law (26) (solid line) as a function of $V = a\chi + c$ in $\ell = 0$ state for α emitters with $Z = 54$–118.

TABLE III. Logarithm of predicted α-decay half-lives $\tau^{(\mathrm{pred})} = \log_{10} T_{\frac{1}{2}}^{(\mathrm{pred})}$ in seconds using formula (26) with parameter $c_f = 0.22$ fixed for $\ell = 0$ and $c_f = 0.1$ for $\ell > 0$. The experimental results of half-lives $\tau^{(\mathrm{expt})} = \log_{10} T_{\frac{1}{2}}^{(\mathrm{expt})}$ in seconds for different ℓs are obtained from Ref. [16]. The α-decay energies Q_α in MeV are taken from atomic mass table of Wang *et al.* [41].

${}^{A}_{Z}$	Q_α	$\tau^{(\mathrm{pred})}$	$\tau^{(\mathrm{expt})}$	ℓ
${}^{144}_{60}$	1.906	23.12	22.86	0
${}^{145}_{60}$	1.579	30.05		0
${}^{145}_{61}$	2.324	17.38	17.30	0
${}^{146}_{61}$	1.909	24.11		2
${}^{147}_{61}$	1.601	30.59		0
${}^{148}_{61}$	1.460	34.36		2
${}^{146}_{62}$	2.5288	15.53	15.51	0
${}^{147}_{62}$	2.3112	18.41	18.52	0
${}^{148}_{62}$	1.9869	23.58	23.34	0
${}^{149}_{62}$	1.8718	25.72		0
${}^{150}_{62}$	1.4504	35.70		0
${}^{130}_{63}$	2.9500	11.88		0
${}^{131}_{63}$	3.0900	10.60		2
${}^{132}_{63}$	3.1400	10.06		0
${}^{133}_{63}$	3.2200	9.46		3
${}^{134}_{63}$	3.0400	10.95		0
${}^{135}_{63}$	3.3500	8.33		3
${}^{136}_{63}$	2.9600	12.02		4
${}^{137}_{63}$	2.8600	13.33		5
${}^{138}_{63}$	2.5600	15.73		1
${}^{139}_{63}$	2.2000	21.72		5
${}^{140}_{63}$	1.7700	29.62		5
${}^{141}_{63}$	1.7220	29.99		0
${}^{148}_{63}$	2.6920	14.38	14.72	0
${}^{151}_{63}$	1.9650	24.96	26.20	2
${}^{134}_{64}$	3.7800	5.67		0
${}^{135}_{64}$	3.4200	7.98		1
${}^{136}_{64}$	3.5700	7.15		0
${}^{137}_{64}$	3.5900	7.04		2
${}^{138}_{64}$	3.2900	9.36		0
${}^{139}_{64}$	2.8000	13.73		1
${}^{140}_{64}$	2.6000	16.39		0
${}^{141}_{64}$	2.3800	19.90		5
${}^{142}_{64}$	2.1100	23.40		0
${}^{143}_{64}$	1.7200	31.07		0
${}^{148}_{64}$	3.2712	9.38	9.37	0
${}^{149}_{64}$	3.1000	10.91	13.27	0
${}^{150}_{64}$	2.8080	13.84	13.75	0
${}^{151}_{64}$	2.6531	15.59	15.03	0
${}^{152}_{64}$	2.2049	21.73	21.53	0
${}^{153}_{64}$	1.8283	28.63		2
${}^{136}_{65}$	3.7400	6.56		0
${}^{137}_{65}$	3.8400	5.85		0
${}^{138}_{65}$	3.5700	7.78		0
${}^{139}_{65}$	3.5900	7.62		0
${}^{140}_{65}$	3.3400	9.61		0
${}^{141}_{65}$	3.1500	11.58		4
${}^{142}_{65}$	2.7700	15.77		5

TABLE III. (*Continued*.)

$^{A}_{Z}$	Q_α	$\tau^{(\mathrm{pred})}$	$\tau^{(\mathrm{expt})}$	ℓ
$^{144}_{65}$	2.1900	22.97		0
$^{145}_{65}$	1.2000	48.10		2
$^{149}_{65}$	4.0778	4.18	4.97	2
$^{150}_{65}$	3.5870	7.54		2
$^{151}_{65}$	3.4970	8.22	8.82	2
$^{152}_{65}$	3.1600	11.32		4
$^{154}_{65}$	2.2100	23.14		5
$^{138}_{66}$	3.9500	5.72		0
$^{139}_{66}$	4.2300	4.03		3
$^{140}_{66}$	3.8400	6.43		0
$^{141}_{66}$	3.4100	9.34		1
$^{142}_{66}$	3.1100	12.37		0
$^{143}_{66}$	3.0400	13.63		5
$^{144}_{66}$	2.7870	15.72		0
$^{145}_{66}$	2.5570	18.51		0
$^{146}_{66}$	1.9800	27.60		0
$^{147}_{66}$	1.6100	35.89		0
$^{149}_{66}$	2.8000	15.61		3
$^{150}_{66}$	4.3512	3.07	3.08	0
$^{151}_{66}$	4.1795	4.07	4.28	0
$^{152}_{66}$	3.7260	7.07	6.93	0
$^{153}_{66}$	3.5590	8.32	8.39	0
$^{154}_{66}$	2.9450	13.85	13.98	0
$^{155}_{66}$	2.6080	17.77		2
$^{156}_{66}$	1.7530	32.25		0
$^{140}_{67}$	4.3700	3.69		0
$^{141}_{67}$	4.1800	4.85		2
$^{142}_{67}$	3.9900	6.01		0
$^{143}_{67}$	3.6600	8.34		0
$^{144}_{67}$	3.4500	10.00		0
$^{145}_{67}$	3.0000	14.45		4
$^{147}_{67}$	2.2400	23.94		0
$^{148}_{67}$	1.9500	29.14		0
$^{149}_{67}$	2.2100	25.02		5
$^{150}_{67}$	3.3900	10.06		1
$^{151}_{67}$	4.6950	2.26		5
$^{152}_{67}$	4.5073	2.74		0
$^{153}_{67}$	4.0520	5.97		5
$^{154}_{67}$	4.0410	5.50	6.57	0
$^{155}_{67}$	3.1590	12.49		2
$^{156}_{67}$	2.8100	16.13		2
$^{157}_{67}$	2.0570	26.61		1
$^{145}_{68}$	3.8800	7.88		5
$^{146}_{68}$	3.3700	11.34		0
$^{147}_{68}$	3.1400	13.46		0
$^{148}_{68}$	2.6660	18.71		0
$^{149}_{68}$	2.0760	27.67		0
$^{150}_{68}$	2.2990	23.85		0
$^{151}_{68}$	3.5050	10.21		3
$^{152}_{68}$	4.9344	1.09	1.06	0
$^{153}_{68}$	4.8023	1.73	1.85	0
$^{154}_{68}$	4.2796	4.60	4.68	0
$^{155}_{68}$	4.1180	5.59	6.16	0

TABLE III. (*Continued*.)

$^{A}_{Z}$	Q_α	$\tau^{(\mathrm{pred})}$	$\tau^{(\mathrm{expt})}$	ℓ
$^{156}_{68}$	3.4830	10.23		0
$^{157}_{68}$	3.3280	11.61	0	2
$^{158}_{68}$	2.6650	18.58		0
$^{159}_{68}$	2.1700	25.86		0
$^{160}_{68}$	2.0390	28.22		0
$^{161}_{68}$	1.7980	33.23		0
$^{162}_{68}$	1.6480	36.90		0
$^{164}_{68}$	1.3040	47.62		0
$^{153}_{69}$	5.2482	0.13	0.21	0
$^{154}_{69}$	5.0938	0.83		0
$^{155}_{69}$	4.5720	3.47	3.06	0
$^{156}_{69}$	4.3450	4.76	5.12	0
$^{157}_{69}$	3.8510	8.53		5
$^{158}_{69}$	3.5110	10.65		0
$^{159}_{69}$	3.0400	15.04		0
$^{160}_{69}$	2.7500	18.58		4
$^{161}_{69}$	2.5100	21.07		1
$^{162}_{69}$	2.2900	25.31		5
$^{163}_{69}$	2.1760	26.73		3
$^{164}_{69}$	2.0530	29.15		4
$^{165}_{69}$	1.8428	33.33		3
$^{154}_{70}$	5.4742	−0.36	−0.36	0
$^{155}_{70}$	5.3387	0.21	0.30	0
$^{156}_{70}$	4.8110	2.72	2.42	0
$^{157}_{70}$	4.6220	3.72	3.89	0
$^{158}_{70}$	4.1700	6.42	6.63	0
$^{159}_{70}$	3.9450	7.98		2
$^{160}_{70}$	3.6210	10.38		0
$^{161}_{70}$	3.1250	14.87		0
$^{162}_{70}$	3.0520	15.61		0
$^{163}_{70}$	2.8360	18.01		0
$^{164}_{70}$	2.6220	20.69		0
$^{165}_{70}$	2.4800	22.70		2
$^{166}_{70}$	2.3130	25.19		0
$^{167}_{70}$	2.1510	27.94		0
$^{168}_{70}$	1.9352	32.15		0
$^{170}_{70}$	1.7359	36.73		0
$^{155}_{71}$	5.8027	−1.23		0
$^{156}_{71}$	5.5960	-0.41		0
$^{157}_{71}$	5.1077	2.22		5
$^{158}_{71}$	4.7900	3.35		0
$^{159}_{71}$	4.4900	5.49		5
$^{160}_{71}$	4.1300	7.26		0
$^{161}_{71}$	3.7500	10.00		0
$^{162}_{71}$	3.4500	12.52		2
$^{163}_{71}$	3.3500	13.42		2
$^{164}_{71}$	3.2300	14.50		0
$^{165}_{71}$	3.0300	16.81		4
$^{167}_{71}$	2.8000	19.44		4
$^{168}_{71}$	2.4100	25.07		5
$^{169}_{71}$	2.4200	24.61		4
$^{170}_{71}$	2.1560	28.80		2
$^{171}_{71}$	2.2892	26.68		4

TABLE III. (*Continued*.)

$^{A}_{Z}$	Q_α	$\tau^{(\text{pred})}$	$\tau^{(\text{expt})}$	ℓ
$^{172}_{71}$	2.1503	28.47		1
$^{173}_{71}$	1.9681	32.66		4
$^{174}_{71}$	1.7992	36.16		0
$^{156}_{72}$	6.0280	−1.64	−1.63	0
$^{157}_{72}$	5.8800	−1.09	−0.91	0
$^{159}_{72}$	5.2250	1.69		0
$^{160}_{72}$	4.9023	3.27	2.77	0
$^{161}_{72}$	4.6850	4.46		2
$^{162}_{72}$	4.4160	5.99	5.80	0
$^{163}_{72}$	4.1500	7.73		2
$^{164}_{72}$	3.9220	9.29		0
$^{165}_{72}$	3.7800	10.39		2
$^{166}_{72}$	3.5400	12.31		0
$^{167}_{72}$	3.4100	13.50		2
$^{168}_{72}$	3.2300	15.17		0
$^{169}_{72}$	3.1500	15.97		0
$^{170}_{72}$	2.9170	18.52		0
$^{171}_{72}$	2.7350	20.38		1
$^{172}_{72}$	2.7540	20.48		0
$^{173}_{72}$	2.5400	23.45		3
$^{174}_{72}$	2.4932	24.04	22.80	0
$^{175}_{72}$	2.3993	25.51		2
$^{176}_{72}$	2.2528	27.88		0
$^{177}_{72}$	2.2443	28.05		2
$^{178}_{72}$	2.0830	30.96		0
$^{157}_{73}$	6.3550	−1.99		5
$^{158}_{73}$	6.1240	−1.57		0
$^{159}_{73}$	5.6810	0.58	0.11	5
$^{160}_{73}$	5.4510	1.14		0
$^{161}_{73}$	5.3300	1.68		0
$^{162}_{73}$	5.0100	2.85	3.68	1
$^{163}_{73}$	4.7490	4.60		0
$^{164}_{73}$	4.5600	5.30		1
$^{165}_{73}$	4.2900	7.39		3
$^{166}_{73}$	4.3100	6.82		1
$^{167}_{73}$	4.0200	9.19		2
$^{168}_{73}$	3.8200	10.68		2
$^{169}_{73}$	3.7300	11.38		2
$^{170}_{73}$	3.4600	13.72		3
$^{171}_{73}$	3.3600	14.21		1
$^{172}_{73}$	3.3100	15.11		3
$^{173}_{73}$	3.2630	15.13		1
$^{174}_{73}$	3.1400	16.97		4
$^{175}_{73}$	2.9960	18.30		0
$^{179}_{73}$	2.3829	26.56		0
$^{158}_{74}$	6.6130	−2.84		0
$^{159}_{74}$	6.4500	−2.30	−2.09	0
$^{160}_{74}$	6.0650	−0.92	−0.99	0
$^{161}_{74}$	5.9230	−0.38		0
$^{162}_{74}$	5.6773	0.62	0.46	0
$^{163}_{74}$	5.5200	1.31	0.83	2
$^{164}_{74}$	5.2785	2.39	2.38	0
$^{165}_{74}$	5.0290	3.61		0

TABLE III. (*Continued*.)

$^{A}_{Z}$	Q_α	$\tau^{(\text{pred})}$	$\tau^{(\text{expt})}$	ℓ
$^{166}_{74}$	4.8560	4.51	4.74	0
$^{167}_{74}$	4.7400	5.14		0
$^{168}_{74}$	4.5000	6.54		0
$^{169}_{74}$	4.2900	7.87		0
$^{170}_{74}$	4.1400	8.88		0
$^{171}_{74}$	3.9600	10.16		0
$^{172}_{74}$	3.8400	11.07		0
$^{173}_{74}$	3.5600	13.39		0
$^{174}_{74}$	3.6000	13.03		0
$^{175}_{74}$	3.3700	15.19		3
$^{176}_{74}$	3.3400	15.40		0
$^{177}_{74}$	3.2900	15.88		0
$^{178}_{74}$	3.0120	18.83		0
$^{179}_{74}$	2.7620	21.92		2
$^{180}_{74}$	2.5150	25.33	25.75	0
$^{181}_{74}$	2.2050	30.12		1
$^{160}_{75}$	6.6980	−2.72	−2.02	0
$^{161}_{75}$	6.3280	−1.46		0
$^{162}_{75}$	6.2400	−1.15	−0.96	0
$^{163}_{75}$	6.0120	−.29	−0.22	0
$^{164}_{75}$	5.9260	0.04		0
$^{165}_{75}$	5.6330	1.25		0
$^{166}_{75}$	5.4600	1.65		1
$^{167}_{75}$	5.2670	3.33		5
$^{168}_{75}$	5.0630	3.95		2
$^{169}_{75}$	5.0140	4.19		2
$^{170}_{75}$	4.7600	5.73		4
$^{171}_{75}$	4.6800	6.04		3
$^{172}_{75}$	4.4400	7.44		0
$^{173}_{75}$	4.3100	7.91		1
$^{174}_{75}$	4.0400	10.15		0
$^{175}_{75}$	4.0100	10.36		0
$^{176}_{75}$	3.8400	11.66		0
$^{177}_{75}$	3.7000	12.80		0
$^{178}_{75}$	3.6600	13.12		0
$^{179}_{75}$	3.4000	15.51		2
$^{180}_{75}$	3.1000	18.56		0
$^{181}_{75}$	2.7710	22.57		2
$^{183}_{75}$	2.1240	32.98		2
$^{184}_{75}$	2.2870	29.95		3
$^{185}_{75}$	2.1941	31.60		2
$^{186}_{75}$	2.0777	33.89		2
$^{162}_{76}$	6.7670	−2.55	−2.73	0
$^{163}_{76}$	6.6800	−2.28		0
$^{164}_{76}$	6.4790	−1.60		0
$^{165}_{76}$	6.3400	−1.11		0
$^{166}_{76}$	6.1390	−0.37	−0.52	0
$^{167}_{76}$	5.9800	0.25		0
$^{168}_{76}$	5.8161	0.91	0.62	0
$^{169}_{76}$	5.7130	1.34	1.59	0
$^{170}_{76}$	5.5368	2.11	1.79	0
$^{171}_{76}$	5.3710	2.89	2.69	2
$^{172}_{76}$	5.2240	3.57	3.91	0

TABLE III. (*Continued.*)

$^{A}_{Z}$	Q_α	$\tau^{(\text{pred})}$	$\tau^{(\text{expt})}$	ℓ
$^{173}_{76}$	5.0550	4.42	5.03	0
$^{174}_{76}$	4.8700	5.41	5.34	0
$^{175}_{76}$	4.5600	7.22		0
$^{176}_{76}$	4.5700	7.15		0
$^{177}_{76}$	4.3500	8.57		2
$^{178}_{76}$	4.2600	9.14		0
$^{179}_{76}$	4.1900	9.61		0
$^{180}_{76}$	3.8500	12.17		0
$^{181}_{76}$	3.7300	13.14		0
$^{182}_{76}$	3.3750	16.38		0
$^{183}_{76}$	3.2100	17.70		1
$^{184}_{76}$	2.9570	20.92		0
$^{185}_{76}$	3.0190	20.65		5
$^{186}_{76}$	2.8204	22.62	22.80	0
$^{187}_{76}$	2.7213	23.93		0
$^{188}_{76}$	2.1434	33.44		0
$^{189}_{76}$	1.9766	36.94		0
$^{164}_{77}$	6.9700	−2.82		0
$^{165}_{77}$	6.8200	−2.34		0
$^{166}_{77}$	6.7220	−2.03	−1.95	0
$^{167}_{77}$	6.5048	−1.29		0
$^{168}_{77}$	6.3810	−0.85		0
$^{169}_{77}$	6.1410	0.04	0.11	0
$^{170}_{77}$	6.1100	0.15	0.08	0
$^{171}_{77}$	6.0010	0.96		5
$^{172}_{77}$	5.9910	0.62		2
$^{173}_{77}$	5.7160	1.78		3
$^{174}_{77}$	5.6240	2.17		2
$^{175}_{77}$	5.4300	3.05	3.02	2
$^{176}_{77}$	5.2400	3.95	2.60	0
$^{177}_{77}$	5.0800	4.77	4.70	0
$^{178}_{77}$	5.0000	5.18		0
$^{179}_{77}$	4.7840	6.38		0
$^{180}_{77}$	4.6600	7.13		2
$^{181}_{77}$	4.3700	8.95		0
$^{182}_{77}$	4.1800	10.25		0
$^{183}_{77}$	3.9600	11.53		1
$^{184}_{77}$	3.8000	13.37		4
$^{185}_{77}$	3.7600	13.13		1
$^{186}_{77}$	3.8500	12.76		2
$^{187}_{77}$	3.8370	12.85		2
$^{188}_{77}$	3.4480	16.31		2
$^{189}_{77}$	2.9410	21.85		2
$^{190}_{77}$	2.7501	24.51		4
$^{191}_{77}$	2.0828	35.63		2
$^{166}_{78}$	7.2860	−3.42		0
$^{167}_{78}$	7.1600	−3.05		0
$^{168}_{78}$	6.9900	−2.52	−2.70	0
$^{169}_{78}$	6.8580	−2.09		2
$^{170}_{78}$	6.7070	−1.61	−1.85	0
$^{171}_{78}$	6.6070	−1.27	−1.35	0
$^{172}_{78}$	6.4640	−0.77		0
$^{173}_{78}$	6.3500	−0.35	−0.36	2

TABLE III. (*Continued.*)

$^{A}_{Z}$	Q_α	$\tau^{(\text{pred})}$	$\tau^{(\text{expt})}$	ℓ
$^{174}_{78}$	6.1830	0.27	0.03	0
$^{175}_{78}$	6.1781	0.29	1.73	2
$^{176}_{78}$	5.8850	1.46	1.22	0
$^{177}_{78}$	5.6428	2.52	2.33	0
$^{178}_{78}$	5.5720	2.83	2.45	0
$^{179}_{78}$	5.4120	3.59		2
$^{180}_{78}$	5.2400	4.42	4.24	0
$^{181}_{78}$	5.1500	4.87	4.86	0
$^{182}_{78}$	4.9510	5.94		0
$^{183}_{78}$	4.8220	6.66	7.48	0
$^{184}_{78}$	4.5980	8.00		0
$^{185}_{78}$	4.4370	9.45		5
$^{186}_{78}$	4.3200	9.81		0
$^{187}_{78}$	4.5500	8.30		3
$^{188}_{78}$	4.0030	12.12	12.53	0
$^{189}_{78}$	3.9000	12.95		2
$^{190}_{78}$	3.2500	18.99	19.31	0
$^{191}_{78}$	3.0950	20.74		2
$^{192}_{78}$	2.4220	30.10		0
$^{193}_{78}$	2.0810	36.59		2

nucleus, our formula (26) can provide the results of α-decay half-life for all types of α-emitting nuclei: even-odd, odd-even, or odd-odd nuclei with the specified ℓ values. The Q_α values of several such α emitters are obtained from Ref. [39] and used in formula (26) to estimate the values of α-decay half-lives. We present these results in Table III as $\tau^{(\text{pred})} = \log_{10} T^{(\text{pred})}_{\frac{1}{2}}$ and compare them with the available experimental results denoted as $\tau^{(\text{expt})} = \log_{10} T^{(\text{expt})}_{\frac{1}{2}}$ in the same Table III. On comparison, we find that our predicted results, $\tau^{(\text{pred})}$, of decay rate are quite close to the corresponding measured values, $\tau^{(\text{expt})}$, both for $\ell = 0$ and $\ell > 0$ states of emission in almost all cases of nuclei. In the same Table III, we have listed the cases of nuclei for which experimental data of decay half-lives are not known. For these nuclei, the results of α-decay half-lives are predicted by (26) using Q_α values obtained from the atomic mass table of Wang *et al.* [41]. These predicted results, $\tau^{(\text{pred})}$, may be useful for future experiments and identification. It may be pointed out here that the Q_α values obtained from Ref. [41] for the nuclei mentioned in Table III are slightly different from the values of some similar nuclei presented in Table II, which are derived from the nuclear mass table by Audi *et al.* [37,38].

For α emission from a deformed nucleus, one can consider for the daughter nucleus a Fermi density distribution with quadrupole deformation and for the α particle a spherical Gaussian shape in the folding calculation [42,43]. The resulting deformed double-folded potential with different quadrupole deformations can be carefully simulated by our versatile potential expression (13). The exact resonance wave function corresponding to this potential can be readily used in the expression (7) for the estimate of decay widths and hence the half-lives in deformed emitters of α cluster. We pursue this investigation and the results will be reported soon.

IV. CONCLUSION

The general formula of the α decay width expressed in terms of regular Coulomb function, resonant wave function, and the difference of potentials is simplified by using the exact wave function at resonance generated by the α + nucleus potential that represents the interaction obtained in the mean-field approximation scheme. From this decay width an extended expression for the decay half-life is derived. Invoking some approximations to different functions in this expression, we obtain a closed formula for the logarithm of half-life in terms of characteristic Q value equal to the resonance energy and the mass and charge numbers of the α emitter. Having all its terms defined, this formula could replace the empirical Viola-Seaborg rule. The calculated results of half-life obtained by using the analytic expression of half-life or the closed formula for the logarithm of the half-life are shown to explain the corresponding measured data with values ranging from 10^{-6} s to 10^{22} y in the cases of large number of α emitters that include heavy and superheavy nuclei. The rectilinear alignment of the logarithm of the experimental decay half-lives as a function of the Viola-Seaborg parameter is reproduced by our analytic expression of logarithm of decay half-lives as a perfectly straight line to mark the excellent explanation of the measured data. Further, having known the Q_α value from the atomic mass tables at a given state of emission and the mass, A_D, and charge, Z_D, numbers of the daughter nucleus, our closed formula (26) can predict the results of α-decay half-life for all types of α-emitting nuclei: even-odd, odd-even, or odd-odd nuclei with the specified ℓ values.

[1] G. Gamow, Z. Phys. **51**, 204 (1928).
[2] H. Geiger and J. Nuttall, Philos. Mag. **23**, 439 (1912).
[3] D. N. Poenaru, I. H. Polonski, R. A. Gherghescu, and W. Greiner, J. Phys. G: Nucl. Part. Phys. **32**, 1223 (2006).
[4] D. N. Basu, J. Phys. G: Nucl. Part. Phys. **30**, B35 (2004).
[5] C. Samanta, P. R. Chowdhury, and D. N. Basu, Nucl. Phys. A **789**, 142 (2007).
[6] P. R. Chowdhury, C. Samanta, and D. N. Basu, Phys. Rev. C **73**, 014612 (2006).
[7] M. Horoi, B. A. Brown, and A. Sandulescu, J. Phys. G: Nucl. Part. Phys. **30**, 945 (2004).
[8] H. Hassanabadi, E. Javadimanesh, and S. Zarrinkamar, Int. J. Mod. Phys. E **22**, 1350080 (2013).
[9] J. Rasmussen, *α-, β-, and γ-Ray Spectroscopy* (North-Holland, Amsterdam, 1966), p. 701.
[10] E. Roeckl, *Nuclear Decay Modes* (Institute of Physics, London, 1996), pp. 237–274.
[11] D. Delion, *Theory of Particle and Cluster Emission*, Lecture Notes in Physics Vol. 819 (Springer-Verlag, Berlin, 2010).
[12] B. Buck, A. C. Merchant, and S. M. Perez, At. Data Nucl. Data Tables **54**, 53 (1993).
[13] S. B. Duarte *et al.*, At. Data Nucl. Data Tables **80**, 235 (2002).
[14] N. Dasgupta-Schubert and M. A. Reyes, At. Data Nucl. Data Tables **93**, 907 (2007).
[15] P. Roy Chowdhury, C. Samanta, and D. N. Basu, At. Data Nucl. Data Tables **94**, 781 (2008).
[16] V. Yu. Denisov and A. A. Khundenko, At. Data Nucl. Data Tables **95**, 815 (2009).
[17] I. Silisteanu and A. I. Budaca, At. Data Nucl. Data Tables **98**, 1096 (2012).
[18] D. S. Delion and A. Dumitrescu, At. Data Nucl. Data Tables **101**, 1 (2015).
[19] V. E. Viola and G. T. Seaborg, J. Inorg. Nucl. Chem. **28**, 741 (1966).
[20] Z. Ren and G. Xu, Phys. Rev. C **36**, 456 (1987); **38**, 1078 (1988).
[21] C. Qi, F. R. Xu, R. J. Liotta, and R. Wyss, Phys. Rev. Lett. **103**, 072501 (2009).
[22] C. Qi, F. R. Xu, R. J. Liotta, R. Wyss, M. Y. Zhang, C. Asawatangtrakuldee, and D. Hu, Phys. Rev. C **80**, 044326 (2009).
[23] C. Qi, A. N. Andreyev, M. Huyse, R. J. Liotta, P. Van Duppen, and R. Wyss, Phys. Lett. B **734**, 203 (2014).
[24] P. Mohr, Phys. Rev. C **73**, 031301 (2006).
[25] B. Sahu, Y. K. Gambhir, and C. S. Shastry, Mod. Phys. Lett. A **25**, 535 (2010).
[26] C. N. Davids and H. Esbensen, Phys. Rev. C **61**, 054302 (2000).
[27] R. G. Lovas, R. J. Liotta, A. Insolia, K. Varga, and D. S. Delion, Phys. Rep. **294**, 281 (1998).
[28] B. Sahu, Phys. Rev. C **78**, 044608 (2008); **84**, 037607 (2011); **85**, 057601 (2012).
[29] B. Sahu, R. Paira, and B. Rath, Nucl. Phys. A **908**, 40 (2013).
[30] D. Ni and Z. Ren, Nucl. Phys. A **825**, 145 (2009).
[31] V. I. Furman, S. Holan, S. G. Kadmensky, and G. Stratan, Nucl. Phys. A **226**, 131 (1974).
[32] S. Mahadevan, P. Prema, C. S. Shastry, and Y. K. Gambhir, Phys. Rev. C **74**, 057601 (2006).
[33] V. P. Bugrov, S. G. Kadmensky, V. I. Furman, and V. G. Khlebostroev, Sov. J. Nucl. Phys. **41**, 717 (1985).
[34] S. Åberg, P. B. Semmes, and W. Nazarewicz, Phys. Rev. C **56**, 1762 (1997); **58**, 3011 (1998).
[35] C. E. Fröberg, Rev. Mod. Phys. **27**, 399 (1955).
[36] G. Royer and H. F. Zhang, Phys. Rev. C **77**, 037602 (2008).
[37] G. Audi, A. H. Wapstra, and C. Thibault, Nucl. Phys. A **729**, 337 (2003).
[38] G. Audi, O. Bersillon, J. Blachot, and A. H. Wapstra, Nucl. Phys. A **729**, 3 (2003).
[39] G. Royer, Nucl. Phys. A **848**, 279 (2010).
[40] Y. Ren and Z. Ren, Phys. Rev. C **85**, 044608 (2012).
[41] M. Wang *et al.*, Chin. Phys. C **36**, 1603 (2012).
[42] D. S. Delion, R. J. Liotta, and R. Wyss, Phys. Rev. C **92**, 051301(R) (2015).
[43] M. Ismail and A. Adel, Phys. Rev. C **89**, 034617 (2014).